Supplementary Material (ESI) for Journal of Materials Chemistry

Monolithic route to efficient dye-sensitized solar cells employing diblock copolymers for mesoporous TiO_2 – Supplementary Information

Mihaela Nedelcu,[†ab] Stefan Guldin,[†a] M. Christopher Orilall,[cd] Jinwoo Lee,[ce] Sven Hüttner,[a] Edward J. W. Crossland,[ag] Scott C. Warren,[cf] Caterina Ducati,[h] Pete R. Laity,[h] Dominik Eder,[h] Ulrich Wiesner,[c] Ullrich Steiner[ag] and Henry J. Snaith,[*i]

a Department of Physics, Cavendish Laboratory, University of Cambridge, J. J. Thomson Avenue, Cambridge CB3 0HE, UK and The Nanoscience Center, Interdisciplinary Research Collaboration in Nanotechnology, University of Cambridge, 11 J. J. Thomson Avenue, Cambridge CB3 0FF, UK.

b current address: Department of Chemistry and Biochemistry, Ludwig-Maximilians-Universität München, Butenandstr. 11, 81377 München, Germany.

c Department of Materials Science and Engineering, Cornell University Ithaca, New York, 14853, USA.

d Current address: NRC Institute for Fuel Cell Innovation, 4250 Wesbrook Mall, Vancouver, B.C. V6T 1W5, Canada.

e Current address: Department of Chemical Engineering and School of Environmental Science and Engineering, Pohang University of Science and Technology, Kyungbuk, 790-784, Korea. item[f] Current address: Ecole Polytechnique Federale de Lausanne, Laboratory of Photonics and Interfaces, 1015 Lausanne, Switzerland.

g Freiburg Institute for Advanced Studies, Albert-Ludwigs-Universität Freiburg (FRIAS), Albertstr. 19, 79104 Freiburg, Germany.

h Department of Materials Science & Metallurgy, University of Cambridge, Cambridge, CB2 3QZ, UK.

i Department of Physics, University of Oxford, OX1 3PU, UK.

† These authors contributed equally to this work.

1 Solar cell performance of 30 µm thick film

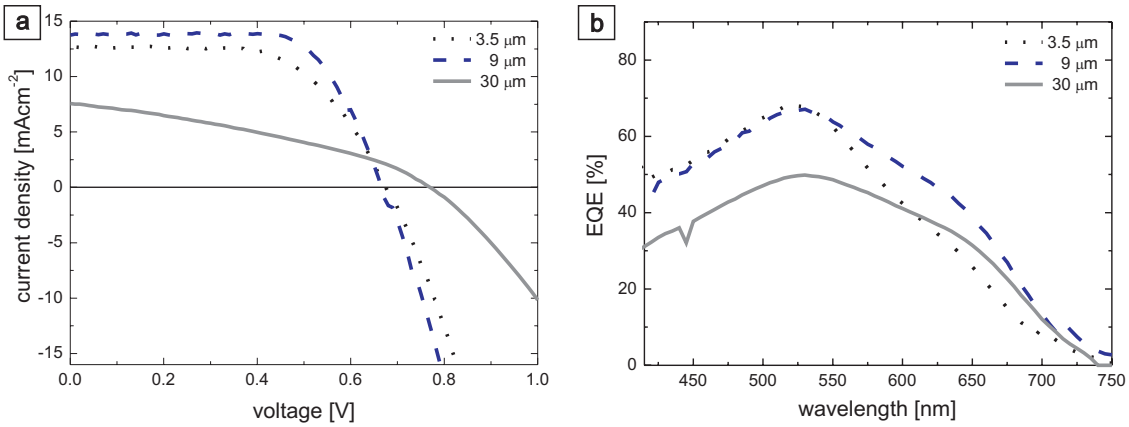

Fig. 1 Liquid electrolyte dye sensitized solar cell performance. (a) Current-voltage, and (b) EQE characteristics for the 30 µm thick device compared to the previously shown cells with TiO_2 layers of 3.5 µm (dotted line) and 9 µm (dashed lined) thickness.

2 Transport and recombination

We have performed transient open-circuit voltage and transient short-circuit photocurrent measurements similarly to as previously described.[1] Here, a single red light emitting diode (630 nm peak) was used as the background and perturbation source, focused to give a maximum intensity of around 100 mWcm^{-2}. The square wave perturbation (1 ms width) was kept to a minimum intensity such that it could be considered small. At open-circuit, when the light pulse hits the device a transient pulse in the voltage is observed. This voltage signal is recorded through the high impedance port (1 MΩ) of an Agilent Technologies oscilloscope. The photoinduced increase in charge density within the active layer causes the increase in voltage. Since the perturbation is small, the transient decay of the voltage is directly proportional to the transient decay of the charge density, allowing an estimate of the electron-hole recombination lifetime. At short-circuit, charge can be collected from the device. Following the light pulse there is a transient pulse observed in the short-circuit current. The transient short-circuit photocurrent is recorded through the low impedance port (50 Ω). The current collection rate is then estimated from the decay of this signal. Due to the use of a red light source, the adsorption can be considered uniform over the entire film, and in essence this experiment corresponds to a 'spatially intergrated' time of flight transient current measurement under zero (low) field. The effective diffusion coefficient for electrons (D_e) can be calculated following $D_e = w^2/2.35\tau_e$, where w is the film thickness and τ_e is the current collection lifetime.

Figure S2 shows the transient signal of the current and voltage perturbation under short-circuit conditions. Here, a sourcemeter (or a galvinostat) is used to allow a constant current, equivalent to short-circuit current, to flow through the circuit. For measuring the voltage perturbation at short-circuit, a Keithley 237 sourcemeter was connected in series with the solar cell, and used to hold the current constant, and equivalent to short-circuit current under the bias light, following a light pulse. The voltage perturbation across the solar cell is recorded by connecting this circuit in parallel with the high impedance port on the oscilloscope, i.e. measuring the voltage perturbation across the solar cell when no extra current is allowed to flow following the light pulse. Following the light pulse the current cannot alter, therefore a voltage perturbation occurs. Since no 'extra' charge can be collected the charge injected from the pulse must recombine within the device and the decay of the voltage perturbation is proportional to the decay of the extra charge in the system, hence the charge lifetime is extracted. In Fig. S2 we show the current and voltage transient responses at short-circuit. Here, we see that the voltage decay is significantly slower than the current decay.

It is possible to estimate the electron diffusion length (L_{D}) from the simple relationship between electron lifetime and diffusion coefficient, $L_{\mathrm{D}} = \sqrt{D_{\mathrm{e}}\tau_{\mathrm{e}}}$. From the data presented, this is estimated to be 18 µm which is in very good agreement with our solar cell thickness dependence measurement and confirming our suspicion that the current collection in the 30 µm thick solar cell is limited by electron hole recombination.

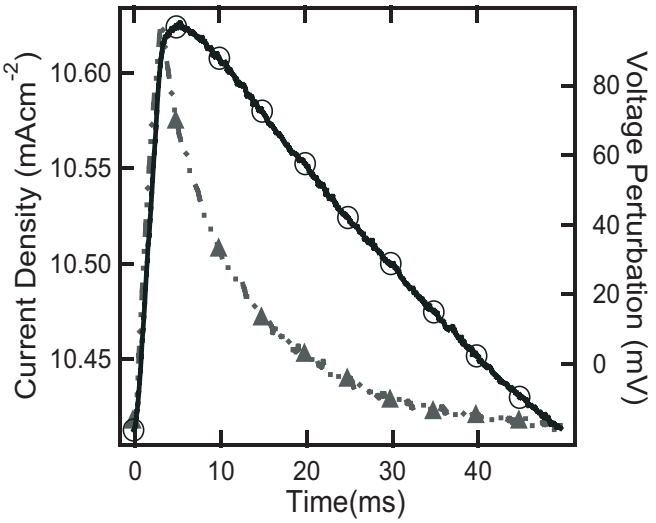

Fig. S2 The current decay lifetime and charge recombination lifetime. Transient signal of the current and voltage perturbation under short-circuit conditions under approximately 100 mWcm^{-2} red light intensity.

3 Analysis of small-angle X-ray data

The data exhibiting a scattering peak was fitted using a model in the form

$$I(q) = S(q) \cdot P(q) \tag{1}$$

This model treats the physical structure as composed of scattering bodies convoluted with a structure factor, which discribes their positions. The scattering is related to the physical structure, as described by the electron density function $\rho_{\mathrm{e}}(\boldsymbol{r})$, through a Fourier transform

$$I(q) = \left| \int_0^\infty \rho_{\mathrm{e}}(\boldsymbol{r}) e^{-iq\boldsymbol{r}} \mathrm{d}\boldsymbol{r} \right|^2 \tag{2}$$

Hence, it can be described by the product of the individual Fourier transforms describing the scattering bodies and the lattice, $S(q)$ and $P(q)$ respectively, as described by Roe[2] and originally proposed by Zernike and Prins.[3] Assuming a (physical) structure in the form of a one-dimensional, distorted lattice, with average periodicity and degree of distortion d and δ respectively

$$S(q) = \frac{1 - A^2}{1 - 2A\cos(qd) + A^2} \tag{3}$$

where $A = \exp(-0.5q^2d^2\delta^2)$. The particle scattering function was based on the assumption that the scatterers were effectively spherical, with radius R normally distributed about the mean R_{avg}, and standard deviation σ. Hence

$$P(q) = B \sum_{R_{\mathrm{min}}}^{R_{\mathrm{max}}} F(R) \cdot V(R) \frac{9\left[\sin(qR) - qR\cos(qR)\right]^2}{(qR)^6} \tag{4}$$

where $V(R) = (4/3)\pi R^3$ and $F(R) = (\sqrt{2\pi}\sigma)^{-1}\exp\{-[(R - R_{\mathrm{avg}})/(2\sigma)]^2\}$. The factor B was included to scale the model to the experimental measurements.

The spectra which did not exhibit a scattering peak were analysed in terms of the Debye-Bueche model, relating the scattered intensity to Fourier transform of the autocorrelation function $\gamma(\boldsymbol{r})$

$$I(q) = \int_0^\infty \mathrm{d}\boldsymbol{r}\,\gamma(\boldsymbol{r})\cdot e^{-iq\boldsymbol{r}}. \tag{5}$$

$\gamma(\boldsymbol{r})$ is the self-convolution of electron density $\rho_{\mathrm{e}}(\boldsymbol{r})$

$$\gamma(\boldsymbol{r}) = \int_0^\infty \mathrm{d}\boldsymbol{u}\,\rho_{\mathrm{e}}(\boldsymbol{u})\rho_{\mathrm{e}}(\boldsymbol{r}+\boldsymbol{u}). \tag{6}$$

In the simplest model, the autocorrelation function is described by an exponential

$$\gamma(\boldsymbol{r}) = \exp\left(\frac{-r}{\zeta}\right) \tag{7}$$

where ζ is the characteristic length. This results in a scattering function of

$$I(q) = \frac{A\zeta^3}{(1+\zeta^2q^2)^2} \tag{8}$$

where A is a constant. Hence

$$[I(q)]^{-0.5} = \frac{1+\zeta^2q^2}{A^{\frac{1}{2}}\zeta^{\frac{3}{2}}} \tag{9}$$

Plotting $I(q)^{-\frac{1}{2}}$ *vs.* q^2 results in a straight line with a slope $\sqrt{\zeta/A}$ and intercept $1/\sqrt{A\zeta^3}$, allowing extract ζ.

4 Nitrogen physisorption

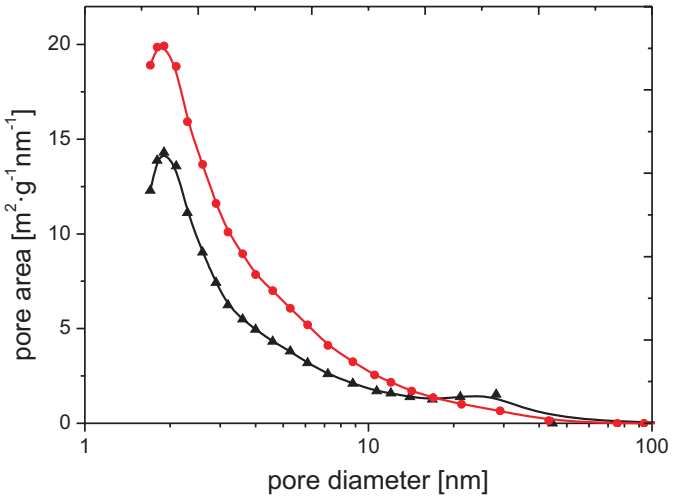

Fig. 2 Nitrogen sorption data of calcined TiO_2 before (triangles) and after (circles) film processing. The plot of pore area vs. pore diameter confirms that the measured specific surface area stems predominately from very small (nanometer-sized) pores, rather than from the mesoscopic (10 nm -sized) morphology.

References

1 H. J. Snaith and M. Graetzel, *Advanced Materials*, 2007, **19**, 3643+.

2 R.-J. Roe, *Methods of X-ray and neutron scattering in polymer science*, Oxford University Press, New York, 2000.

3 F. Zernike and J. Prins, *Z. Physik*, 1927, **41**, 184–194.